Oogenesis requires germ cell-specific transcriptional regulators *Sohlh1* and *Lhx8*

Stephanie A. Pangas*, Youngsok Choi†, Daniel J. Ballow†, Yangu Zhao‡, Heiner Westphal‡, Martin M. Matzuk*§¶, and Aleksandar Rajkovic†‖

Departments of *Pathology, †Obstetrics and Gynecology, §Molecular and Cellular Biology, and ¶Molecular and Human Genetics, Baylor College of Medicine, Houston, TX 77030; and ‡Laboratory of Mammalian Genes and Development, National Institute of Child Health and Human Development, Bethesda, MD 20892

Edited by Brigid L. M. Hogan, Duke University Medical Center, Durham, NC, and approved April 12, 2006 (received for review February 9, 2006)

Mammalian oogenesis requires oocyte-specific transcriptional regulators. The full complement of oocyte-specific transcription factors is unknown. Here, we describe the finding that *Sohlh1*, a spermatogenesis and oogenesis basic helix–loop–helix transcription factor in females, is preferentially expressed in oocytes and required for oogenesis. *Sohlh1* disruption perturbs follicular formation in part by causing down-regulation of two genes that are known to disrupt folliculogenesis: newborn ovary homeobox gene (*Nobox*) and factor in the germ-line alpha (*Figla*). In addition, we show that *Lhx8* is downstream of *Sohlh1* and critical in fertility. Thus, *Sohlh1* and *Lhx8* are two germ cell-specific, critical regulators of oogenesis.

infertility | oocyte | ovary | reproduction | folliculogenesis

Mouse primordial germ cells, at embryonic days 9.5–11.5 (E9.5–E11.5), migrate to the urogenital ridges from the proximal epiblast. Mitotic division of primordial germ cells, coupled with incomplete cytokinesis, results in oocytes in clusters (also called cysts) at ≈E10.5 (1, 2). Female germ cells, at ≈E13.5, begin entry into prophase I of meiosis and arrest in the diplotene stage of the first meiotic division. Oocytes arrested in meiosis I are thought to remain arrested until the time of ovulation. Germ cell clusters formed in the embryonic gonad break down shortly after birth in the mouse. Breakdown of germ cell cysts results in oocytes enveloped by somatic pregranulosa cells (now called primordial follicles) (1). Primordial follicles represent a reservoir of follicles that are recruited periodically to grow into primary and more advanced follicular structures.

The breakdown of germ cell clusters, formation of primordial follicles, and transition to primary follicles represents a critical period of follicle formation. Transcription of numerous oocyte-specific genes, such as growth and differentiation factor 9 (*Gdf9*), bone morphogenetic protein 15 (*Bmp15*), and zona pellucida genes 1–3 (*Zp1–3*) (3–6), commences during early folliculogenesis. Regulation of these genes is in part due to expression of two known oocyte-specific transcription factors, *Figla* (7) and *Nobox* (3). FIGLA is a basic helix–loop–helix transcription factor that regulates expression of the zona pellucida genes (7, 8). *Nobox* is a homeobox gene that is necessary for expression of several key oocyte-specific genes, including *Gdf9*, *Bmp15*, and *Pou5f1* but not *Figla* or *Zp1–3* (3). However, other oocyte-specific transcriptional regulators likely exist, because numerous oocyte-specific genes are not affected by the lack of *Nobox* and *Figla*. Here, we describe our finding that *Sohlh1* and *Lhx8*, which are both preferentially expressed during oogenesis in females, are critical in early folliculogenesis.

Results and Discussion

We identified *Sohlh1* by an *in silico* subtraction strategy to identify genes that are preferentially expressed during early folliculogenesis (9). *Sohlh1* encodes a basic helix–loop–helix transcription factor with homologues in humans and other placental mammals (Fig. 8, which is published as supporting information on the PNAS web site). In females, ovaries preferentially express *Sohlh1* transcripts as shown by multitissue RT-PCR analysis (Fig. 9, which is published as supporting information on the PNAS web site). Embryonic ovaries express readily

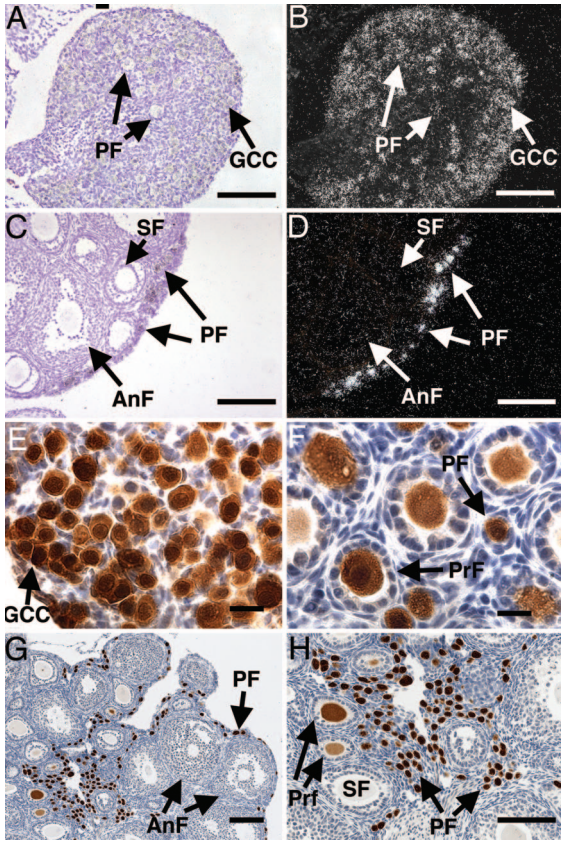

Fig. 1. *Sohlh1* mRNA and protein expression. (*A–D*) *In situ* hybridization with *Sohlh1* riboprobe on newborn (*A* and *B*) and 6-week-old (*C* and *D*) ovarian tissue. Bright-field (*A* and *C*) and dark-field (*B* and *D*) views are shown. Arrows throughout show locations of germ cell cysts (GCC), primordial follicles (PF), primary follicles (PrF), secondary follicles (SF), and antral follicles (AnF). *Sohlh1* transcripts localize mainly to germ cell cysts and oocytes in primordial follicles. (*E–H*) Rabbit antibodies against SOHLH1 were used to perform immunohistochemistry on newborn (*E*), 9-day-old (*F*), and 6-week-old (*G* and *H*) ovaries. Immunoreactivity to the SOHLH1 protein stained brown, and cell nuclei were counterstained blue with hematoxylin. (Scale bars: *A–D* and *G* and *H*, 100 μm; *E* and *F*, 20 μm.)

Conflict of interest statement: No conflicts declared.

This paper was submitted directly (Track II) to the PNAS office.

Abbreviations: E*n*, embryonic day *n*; ChIP, chromatin immunoprecipitation; GCNA1, germ cell nuclear antigen 1.

‖To whom correspondence should be addressed at: Department of Obstetrics and Gynecology, Baylor College of Medicine, 1709 Dryden Road, Suite 1100, Houston, TX 77030. E-mail: rajkovic@bcm.tmc.edu.

www.pnas.org/cgi/doi/10.1073/pnas.0601083103

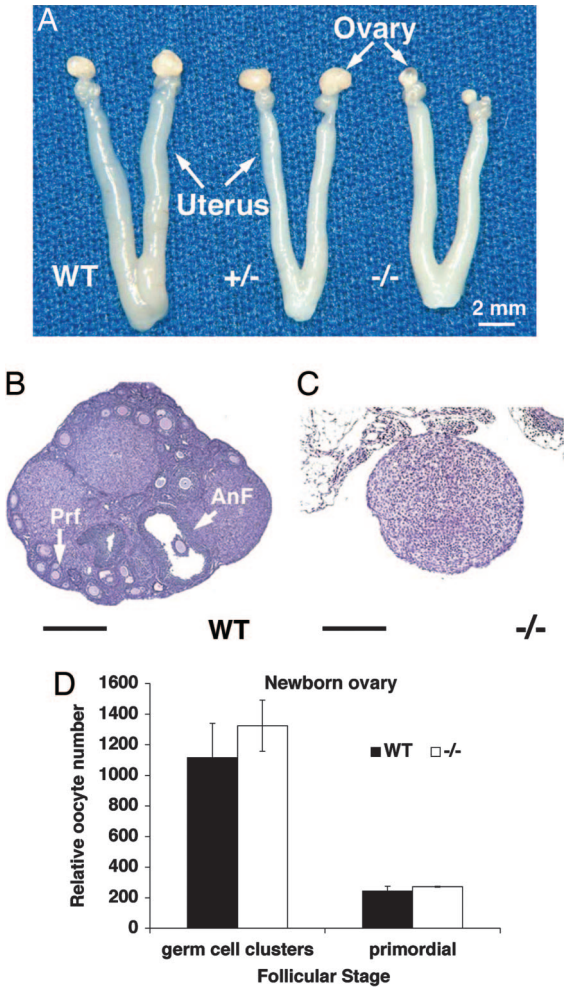

Fig. 2. *Sohlh1* adult knockout anatomy, histology, and histomorphometric analysis. (*A*) Gross reproductive tracts dissected from WT, heterozygous (+/−), and homozygous (−/−) *Sohlh1* mice. Note markedly smaller ovaries in *Sohlh1*$^{-/-}$ mice. (*B*) WT ovary with advanced antral follicle (AnF) as well as primary follicles (Prf). (*C*) *Sohlh*$^{-/-}$ ovary (−/−) lacks germ cells. (*D*) Five pairs of newborn ovaries from WT and *Sohlh1* knockout (−/−) mice were sectioned, and oocytes within the germ cell clusters and primordial follicles were counted. No significant differences were observed between the WT and knockout ovaries. Data are represented as mean values, with error bars representing the SEM. Fisher's exact *t* test was used to calculate *P* values. (Scale bars: 400 μm.)

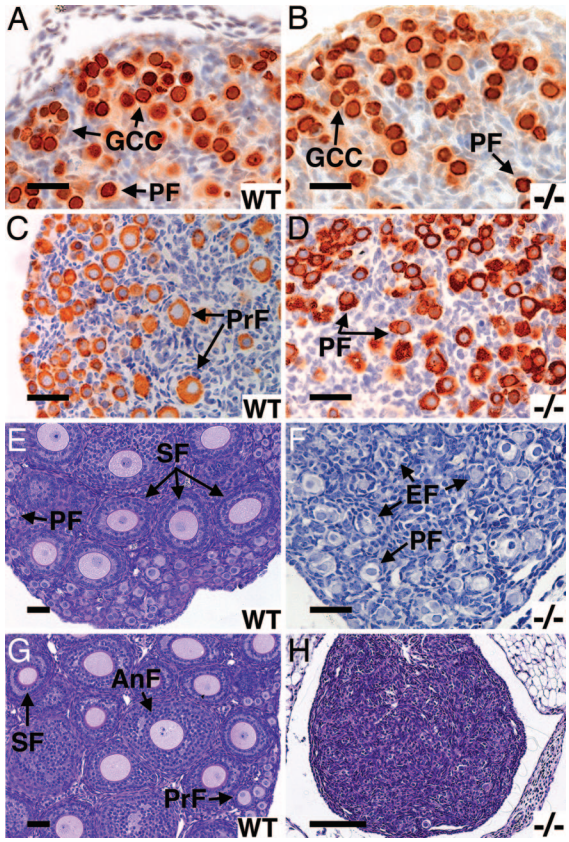

Fig. 3. *Sohlh1* knockout histology and immunohistochemistry; WT and knockout (−/−) data are shown. (*A* and *B*) Newborn ovaries stained with antibodies against GCNA1 show no difference in primordial follicles (PF) or germ cell cysts (GCC) between WT (*A*) and knockout (*B*). (*C* and *D*) Three-day ovaries stained anti-MSY2. Primary follicles (PrF) are seen in WT (*C*) but not knockout (*D*) ovaries. (*E* and *F*) Periodic acid/Schiff reagent (PAS) staining of 7-day WT (*E*) and knockout (*F*) ovaries show fewer follicle types and empty follicles (EF) in the knockout (*F*). (*G* and *H*) PAS staining of 3-week ovaries shows no remaining oocytes in the knockout (*H*) but all stages of development in the WT (*G*). (Scale bars: *A–G*, 50 μm; *H*, 400 μm.)

detectable levels of *Sohlh1* at E15.5, at the time when oocytes have entered meiosis I, although a low level of *Sohlh1* mRNA expression is detectable at E13.5. Newborn mouse ovaries contain oocyte clusters confined to germ cell cysts and primordial follicles. *Sohlh1* transcripts are present in oocytes of germ cell cysts as well as primordial follicles in the newborn ovary (Fig. 1 *A* and *B*). In adult ovaries, *Sohlh1* transcripts are preferentially expressed in primordial oocytes but disappear rapidly as the oocytes are recruited to form primary and secondary (multilayer and preantral) follicles (Fig. 1 *C* and *D*). SOHLH1 protein is detected in germ cell cysts, primordial follicles, and primary follicles but is undetectable by the secondary follicle stage (Fig. 1 *E–H*). SOHLH1 protein lacks the classic nuclear localization signal, and immunohistochemistry shows that SOHLH1 is located both in the nucleus and the cytoplasm. Nuclear chaperoning may therefore regulate SOHLH1 function. The above expression studies show that *Sohlh1* has a RNA and protein expression pattern that differs from other known oocyte-specific transcription regulators, *Nobox* and *Figla*, and suggest that *Sohlh1* plays a unique role in early folliculogenesis.

To define the roles of SOHLH1 in early stages of folliculogenesis, we generated a targeted deletion of the first three exons that encode the SOHLH1 basic helix–loop–helix domain as well as 500 nucleotides upstream of the putative transcription initiation site (10). Heterozygous *Sohlh1*$^{+/-}$ matings produced expected Mendelian ratios, and females averaged 8.1 ± 2.0 pups per litter (n = 45 breeding pairs) over a 6-month period and remained fertile for at least 9 months. Litter sizes were not statistically different from the WT average (8.4 ± 2.0 pups per litter). In contrast, all *Sohlh1*$^{-/-}$ homozygous null females were infertile, with atrophic ovaries that, on histologic examination, lacked oocytes at 10 weeks of age on a C57BL/6J;129S5/SvEvBrd hybrid background (Fig. 2 *A–C*). Adult *Sohlh1*$^{-/-}$ ovaries occupied ≈1/10 of the WT volume.

To determine the onset of histologic changes and germ cell loss, we compared ovarian development in WT and *Sohlh1*$^{-/-}$ mice. Newborn WT and *Sohlh1*$^{-/-}$ ovaries show no apparent differences in morphology or histology, and histomorphometric analysis found no statistically significant differences in the number of oocytes present (Fig. 2*D*). We used antibodies against two germ cell-specific antigens, GCNA1 (germ cell nuclear antigen 1) and MSY2 (germ cell-specific Y box protein), to study oocyte development in WT and mutants. GCNA1 is a nuclear marker for the germ cell lineage. It is expressed in germ cells after their arrival at the gonad until the

DEVELOPMENTAL BIOLOGY

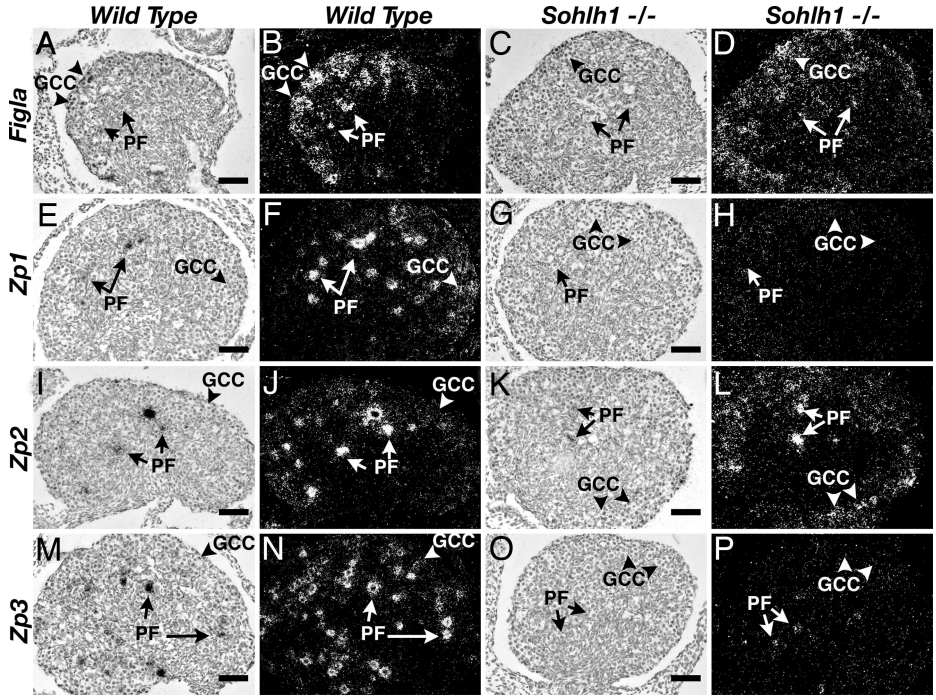

Fig. 4. Expression of *Figla*, *Zp1*, *Zp2*, and *Zp3* in WT and *Sohlh1*$^{-/-}$ ovaries. Bright-field (*A*, *C*, *E*, *G*, *I*, *K*, *M*, and *O*) and their corresponding dark-field (*B*, *D*, *F*, *H*, *J*, *L*, *N*, and *P*) images of *in situ* hybridization from WT (*A*, *B*, *E*, *F*, *I*, *J*, *M*, and *N*) and *Sohlh1*$^{-/-}$ (*C*, *D*, *G*, *H*, *K*, *L*, *O*, and *P*) newborn ovaries. In newborn WT ovaries, *Figla* (*A* and *B*), *Zp1* (*E* and *F*), *Zp2* (*I* and *J*), and *Zp3* (*M* and *N*) are expressed in germ cell cysts (GCC; arrowheads) and primordial follicles (PF; arrows). Expression of *Figla* (*C* and *D*) and *Zp2* (*K* and *L*) are detectable in *Sohlh1*$^{-/-}$ ovaries by *in situ* hybridization. *Zp1* (*G* and *H*) and *Zp3* (*O* and *P*) are not detectable by *in situ* hybridization in *Sohlh1*$^{-/-}$ ovaries. Magnification is the same in *A*–*P*. (Scale bars: 40 μm.)

diplotene/dictyate stage of the first meiotic division (11). Oocytes in primordial follicles and germ cell cysts from WT and *Sohlh1*$^{-/-}$ newborn ovaries stained similarly with anti-GCNA1 antibodies (Fig. 3 *A* and *B*). These data indicate that embryonic germ cell migration and proliferation is grossly normal in newborn *Sohlh1*$^{-/-}$ females. MSY2 is a cytoplasmic marker for oocytes that have entered the diplotene stage and persists in dictyate stages (12, 13). By postnatal day 3, MSY2 immunoreactivity is present in oocytes of primary follicles of WT ovaries (Fig. 3*C*). In contrast, *Sohlh1*$^{-/-}$ ovaries lack primary follicles on postnatal day 3 (Fig. 3*D*), and anti-MSY2 staining is present only in oocytes of primordial follicles. Thus, there appears to be a defect in follicle development during the primordial-to-primary follicle transition.

Secondary follicles develop in WT ovaries by postnatal day 7 (Fig. 3*E*), but, by this time, *Sohlh1*$^{-/-}$ ovaries are significantly smaller than WT, and few oocytes are observed (Fig. 3*F*). Most oocytes in the 7-day-old *Sohlh1*$^{-/-}$ ovaries are still enveloped by flat somatic cells similar to primordial follicles but now also contain multiple empty follicles in the central portion of the ovary (Fig. 3*F*). By 3 weeks of age, *Sohlh1*$^{-/-}$ ovaries contained few germ cells (Fig. 3*H*), although a secondary follicle was occasionally seen, and *Sohlh1*$^{-/-}$ ovaries beyond 7 weeks lacked by histology germ cells and follicular structures. Thus, the time frame for oocyte and follicle loss in *Sohlh1*$^{-/-}$ mutant females is reminiscent of *Figla*$^{-/-}$ and *Nobox*$^{-/-}$ ovaries (3, 7), which also exhibit early postnatal oocyte loss. Similar to *Nobox*$^{-/-}$ ovaries, *Sohlh1*$^{-/-}$ ovaries do not misexpress meiotic genes *Mlh1* and *Msh5* or apoptosis genes *Bax*, *Bcl2*, *Casp 2*, and *Bcl2l2* (data not shown). *Figla*, *Nobox*, and *Sohlh1* oocyte-specific pathways may therefore overlap.

We reported previously that the *Nobox* deficiency did not affect expression of *Figla* and FIGLA's presumed targets, the zona pellucida genes *Zp1*, *Zp2*, and *Zp3* (3). However, *Sohlh1*$^{-/-}$ ovaries contain significantly lower amounts of *Figla* transcripts, as shown by *in situ* hybridization (Fig. 4 *A*–*D*) and quantitative RT-PCR (Fig. 10, which is published as supporting information on the PNAS web site). Ovaries that lack *Figla* form very few primordial follicles (7). *Sohlh1*$^{-/-}$ ovarian pathology is less severe than reported for the *Figla* knockouts, and persistent low levels of *Figla* expression in *Sohlh1*$^{-/-}$ animals may account for this difference in pathology.

By sequence analysis, the *Figla* promoter lacks conserved E box elements and therefore is not likely a direct transcriptional target of *Sohlh1*. FIGLA's target genes, *Zp1* and *Zp3*, are drastically down-regulated in *Sohlh1*$^{-/-}$ ovaries (Figs. 4 *E*–*H* and *M*–*P* and 10) as compared with *Zp2* expression (Figs. 4 *I*–*L* and 10). It is possible that SOHLH1 positively cooperates with FIGLA in the transcriptional regulation of *Zp1* and *Zp3* but not *Zp2* and that, in the absence of SOHLH1, FIGLA is insufficient to activate transcription of *Zp1* and *Zp3*. Alternatively, the 4-fold reduction in *Figla* expression may be more detrimental for transcription of *Zp1* and *Zp3* as compared with *Zp2*. Studies have shown that FIGLA-binding sites in the *Zp2* promoter differ from the *Zp1* and *Zp3* promoter sites (8) and that FIGLA transactivates the *Zp2* promoter 2-fold higher than the promoters of either *Zp1* or *Zp3* (8).

Nobox transcripts are also reduced ≈4-fold in *Sohlh1*$^{-/-}$ ovaries (Fig. 11, which is published as supporting information on the PNAS web site), whereas *Sohlh1* transcripts (AW554400) are not significantly affected in *Nobox*$^{-/-}$ ovaries (3). Oocyte-specific genes that are down-regulated in *Nobox*$^{-/-}$ ovaries, such as *Gdf9*, *Pou5f1*, *Zar1*, *Mos*, and *H1foo*, are also down-regulated in *Sohlh1*$^{-/-}$ ovaries, consistent with the reduction of *Nobox* (Fig. 11 *B*, *C*, and *G*) and confirming that the NOBOX pathway is compromised in *Sohlh1*$^{-/-}$ ovaries. Therefore, NOBOX functions downstream of SOHLH1, and loss of the NOBOX pathway likely contributes to the *Sohlh1*$^{-/-}$ phenotype. Not all germ cell-specific genes are down-regulated; *Nohma* transcript levels are not significantly different in WT and *Sohlh1*$^{-/-}$ newborn ovaries (Fig. 11*D*). *Stra8*, an early molecular marker for female germ cell differentiation (14), disappears in the WT at ≈E16.5, at the time when meiosis is ongoing in female germ cells. *Sohlh1*$^{-/-}$ newborn ovaries, however, express *Stra8* (Fig. 11*E*). The continued expression of *Stra8* and lack of induction of *Pou5f1* in newborn ovaries (Fig. 11) argues that *Sohlh1*$^{-/-}$ newborn oocytes partly retain an embryonic gene expression pattern despite the grossly normal appearance of the newborn ovaries. Moreover, what histologically appear to be primordial oocytes in *Sohlh1*$^{-/-}$ ovaries may not be functional primordial oocytes because of misexpression of multiple oocyte-specific genes.

Because the newborn *Sohlh1*$^{-/-}$ ovarian histology was grossly similar to WT but demonstrated molecular defects, we chose this

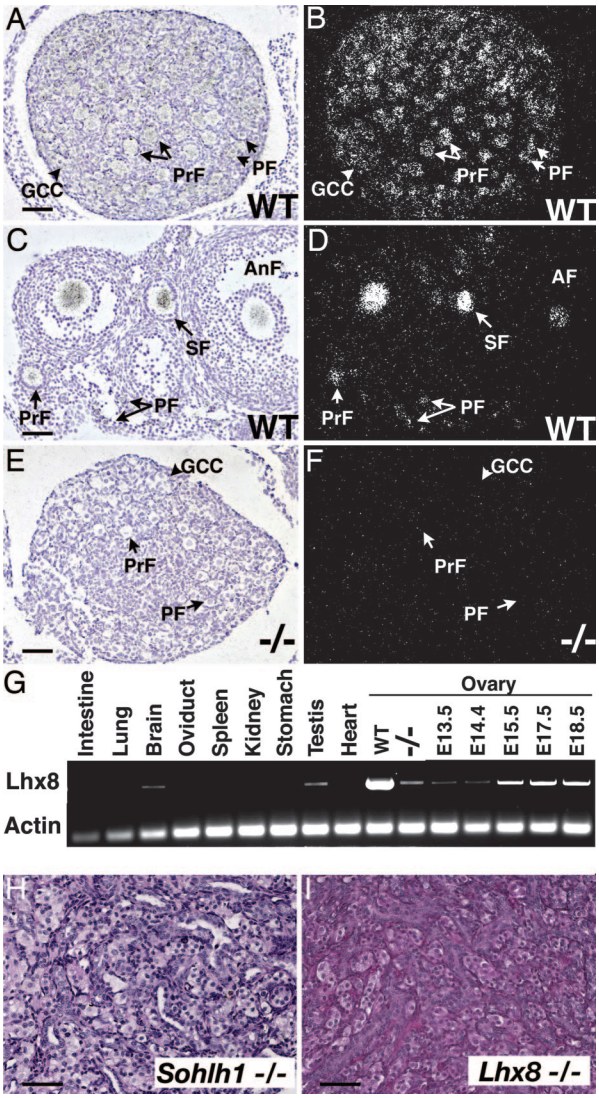

Fig. 5. *Lhx8* expression and ovarian phenotype. (*A–F*) Bright-field (*A*, *C*, and *E*) and dark-field (*B*, *D*, and *F*) views of *in situ* hybridization are shown with *Lhx8* riboprobe to WT newborn (*A* and *B*) and 6-week-old (*C* and *D*) ovaries. (*E* and *F*) The *Lhx8* riboprobe showed no significant hybridization to *Sohlh1*$^{-/-}$ ovaries. (*G*) Oligonucleotides corresponding to *Lhx8* amplified RNA in WT testes and newborn ovaries (WT) but showed a dramatic decrease in *Sohlh1*$^{-/-}$ ovaries (−/−). Total RNA from embryonic ovaries (E13.5, E14.5, E15.5, E17.5, and E18.5) was isolated and also amplified with *Lhx8*-specific primers. (*H* and *I*) Periodic acid/Schiff reagent staining of 12-week old (adult) ovaries from *Sohlh1*$^{-/-}$ (*H*) and *Lhx8*$^{-/-}$ (*I*) shows a lack of germ cells in both mutants. GCC, germ cell cyst; PF, primordial follicle; PrF, primary follicle; SF, secondary follicle; AnF, antral follicle. (Scale bars: 40 μm.)

age for oligonucleotide microarray analysis (data not shown). Microarray analysis indicated that another transcription factor, *Lhx8*, was drastically down-regulated in *Sohlh1*$^{-/-}$ ovaries. *Lhx8* encodes a LIM homeodomain protein (15–17), and because the role of *Lhx8* in reproduction is unknown, we analyzed *Lhx8* expression in ovaries. *Lhx8* transcripts localize to oocytes of germ cell cysts and primordial, primary, and antral follicles (Fig. 5 *A–D*). However, *Lhx8* was not detectable in oocytes of *Sohlh1*$^{-/-}$ ovaries by *in situ* hybridization, and *Lhx8* mRNA is barely detectable by RT-PCR in *Sohlh1*$^{-/-}$ ovaries (Figs. 5 *E–G* and 11*F*). Multitissue RT-PCR with RNA derived from adult tissues shows that *Lhx8* is preferentially expressed in testes and ovaries (Fig. 5*G*). Because *Lhx8* was drastically down-regulated in *Sohlh1*$^{-/-}$ ovaries, we examined *Lhx8*$^{-/-}$ ovaries. Adult *Lhx8*$^{-/-}$ ovaries lack germ cells and appear histologically identical to adult *Sohlh1*$^{-/-}$ ovaries (Fig. 5 *H* and *I*). *Lhx8* mRNA expression is detectable as early as E13.5 and mimics *Sohlh1* embryonic expression (Figs. 5*G* and 9*B*). These results indicate that *Lhx8* is likely downstream of SOHLH1 and that part of the *Sohlh1*$^{-/-}$ phenotype is secondary to disruption in *Lhx8* expression.

The above experiments suggest that *Lhx8*, *Zp1*, *Zp3*, and *Nobox* are candidate genes for direct regulation by SOHLH1. Strictly conserved E box elements are found within the proximal promoters or noncoding regions of these genes (Fig. 12, which is published as supporting information on the PNAS web site). We studied regulation of these promoters by chromatin immunoprecipitation (ChIP) and transient transfection experiments. To identify promoters bound by SOHLH1 *in vivo*, we performed ChIP experiments with protein extracts from newborn mouse ovaries. Extracts were cross-linked, sonicated, and immunoprecipitated with the anti-SOHLH1 antibody. DNA sequences from the *Lhx8*, *Zp1*, and *Zp3* promoters coprecipitated with the anti-SOHLH1 antibody (Fig. 6*A*), suggesting that SOHLH1 binds these regions. In contrast, coimmunoprecipitation was not detected for the *Nobox* or *Zp2* promoters (Fig. 6*A*). Therefore, neither *Nobox* nor *Zp2* is likely a direct target of SOHLH1. To further address the role of SOHLH1 in regulation of the *Lhx8*, *Zp1*, and *Zp3* promoters, we used transient transfection of reporter constructs in HEK293 cells. Cotransfection of a mouse *Sohlh1* expression vector with E box-containing promoter regions of mouse *Lhx8*, *Zp1*, and *Zp3* fused to luciferase resulted in significant transactivation (Fig. 6 *B–D*). Mutation of the E box sequences abolished SOHLH1-dependent stimulation (Fig. 6 *B–D*). Thus, *Lhx8*, *Zp1*, and *Zp3* are likely direct downstream target genes of SOHLH1 through the E box elements in their promoters.

Very little is known about the molecular pathways that direct the development of the female germ cell. The finding that *Sohlh1* and *Lhx8* are necessary in oogenesis adds to the growing number of transcription factors that play critical roles in oocyte development. Our data indicate that SOHLH1 acts upstream of *Lhx8*, *Figla*, and *Nobox*. Of these, *Lhx8* is a direct target gene, as are *Zp1* and *Zp3*. In the embryonic period, the *Sohlh1* and *Lhx8* mRNA expression patterns in oocytes are similar, consistent with *Lhx8* regulation by SOHLH1. However, *Sohlh1* expression postnatally is confined to oocytes of follicles up to the primary follicle stage. This temporally restricted expression pattern is in stark contrast to the postnatal and adult expression patterns of *Lhx8*, *Figla*, *Zp1–3*, and *Nobox*, which are maintained in oocytes of more advanced follicles. Thus, differentiation of primordial oocytes may depend on the transient expression of *Sohlh1* to direct expression of *Lhx8* and perhaps others, which in turn regulate *Nobox* and *Figla* (Fig. 7). These transcription factors may then serve as self-sustaining determinants of oocyte-specific gene expression throughout the remainder of folliculogenesis. In total, our data indicate that *Sohlh1* is an integral part of a genetic program that is required for germ cell-specific gene expression and may be a master regulator during oogenesis. In humans, female infertility due to germ cell loss has few known molecular origins (18). Therefore, *SOHLH1, NOBOX, LHX8, FIGLA* and the genes that they regulate are all important candidate genes for nonsyndromic ovarian failure.

Materials and Methods

Targeting Construct. *Sohlh1* genomic clones were isolated from a 129S6/SvEv genomic library, and a targeting construct was generated (10). The *Sohlh1* targeting construct was electroporated into AB2.2 ES cells to mutate the WT *Sohlh1* locus by homologous recombination as described in ref. 19. The mutant *Sohlh1* allele replaces exons 2–8 with the *Pgk1-HPRT* cassette.

DEVELOPMENTAL BIOLOGY

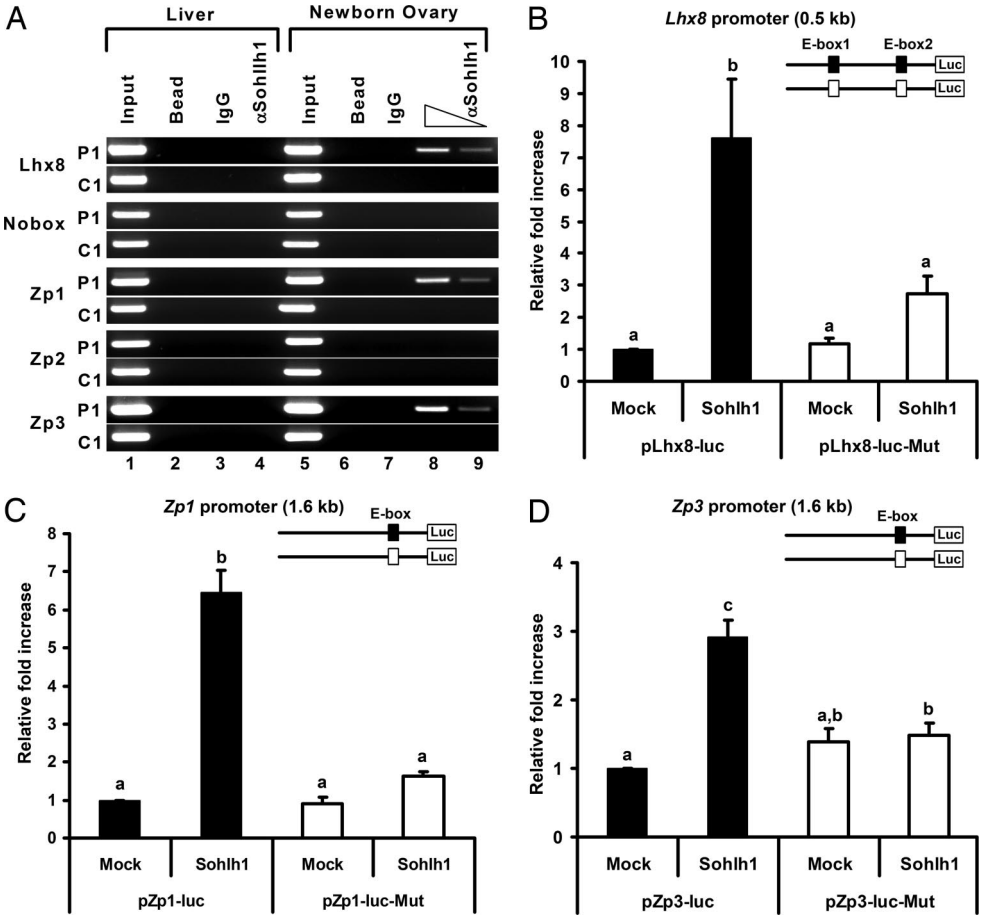

Fig. 6. SOHLH1 binding and transactivation of the *Lhx8*, *Zp1*, and *Zp3* promoters. (*A*) ChIP assays with anti-SOHLH1 antibodies on newborn ovary and liver extracts. Anti-SOHLH1 antibodies precipitate genomic DNA containing conserved E boxes from *Lhx8*, *Zp1*, and *Zp3* promoter regions (P1) but not control genomic regions (C1). PCR amplifications of the E boxes are described in the legend of Fig. 12 and Table 2. "Input" is PCR product from chromatin pellets before immunoprecipitation. Samples incubated with anti-SOHLH1 antibody (αSohlh1) and the control sample without antibody (Bead) or IgG were used as templates for PCR. (*B–D*) Transient transfection analyses of *Lhx8* (*B*), *Zp1* (*C*), and *Zp3* (*D*) promoter regions with SOHLH1. Reporter constructs containing the WT (filled box, pLhx8-luc, pZp1-luc, and pZp3-luc) or mutant E boxes (open box, pLhx8-luc-Mut, pZp1-luc-Mut, and pZp3-luc-Mut) were cotransfected with vector expressing SOHLH1 or the empty vector (Mock). *Lhx8* putative promoter contains two E boxes, and both were mutated. Conserved E boxes and mutated sequences are shown in Fig. 12 and Table 1. The mean fold increase in luciferase activity (± SEM) of triplicate experiments relative to the empty vector is shown. Statistical significance was determined by one-way ANOVA followed by the Tukey–Kramer honestly significant difference test for multiple comparisons. Bars marked with difference letters (a, b, and c) indicate statistical significance ($P < 0.001$).

Breeding, Histology, Histomorphometric Analysis, and Immunohistochemistry. All mouse experiments were carried out on a C57BL/6/129S5/SvEvBrd hybrid background. Litters were weaned at 3 weeks, and breeding pairs were set up at 6 weeks of age. One mating pair was placed per cage and inspected every morning for the presence of litters. For histological analysis, ovaries were placed in 10% buffered formalin, processed, embedded in paraffin, serially sectioned (5 μm), and stained with hematoxylin and eosin or with periodic acid/Schiff reagent and hematoxylin. Five pairs of ovaries of each genotype were subjected to gross and microscopic analysis for each time point. For histomorphometric analysis, every fifth section was derived from the long axis of the ovary and photographed, and oocytes containing nuclei were scored. The total numbers of oocytes from all of the sections were summed, and the mean number per ovary was determined. No correction factor was used. Fisher's exact *t* test was used to calculate *P* values. Adult ovarian volume was calculated by using the ellipse formula, $A \times B \times C \times 0.5233$, where A is the long axis, B is the largest anteroposterior measurement, and C is the largest transverse diameter.

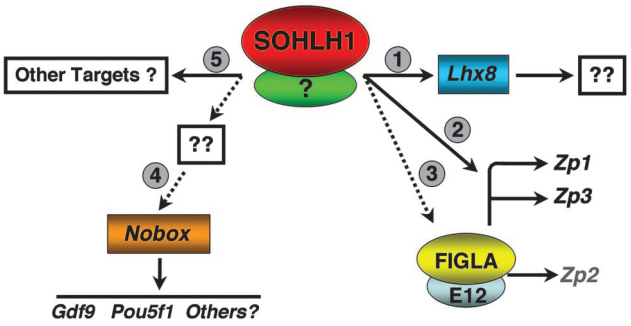

Fig. 7. Hypothetical model for SOHLH1 role in early folliculogenesis. SOHLH1 regulates a number of genes that are required for early oocyte development. The SOHLH1 interacting partner is unknown. (Step 1) The homeobox gene *Lhx8* is likely a direct transcriptional target of SOHLH1, but genes downstream of LHX8 in the oocyte are unknown. (Step 2) *Zp1* and *Zp3* are likely directly regulated by SOHLH1, possibly in conjunction with FIGLA. (Step 3) *Figla* is partially down-regulated in *Sohlh1* null oocytes, but *Zp2*, which is controlled by the FIGLA/E12 complex, is not significantly changed. (Step 4) The oocyte-specific homeobox gene, *Nobox*, is downstream of SOHLH1. Loss of *Nobox* expression in *Sohlh1* null oocytes also results in loss of genes downstream of the NOBOX pathway, such as *Gdf9* and *Pou5f1*. (Step 5) It is likely that SOHLH1 has additional target genes. Dotted lines indicate unknown pathways. Solid lines indicate direct transcriptional regulation.

Germ cell cysts were defined as two or more oocytes that were not individually separated by stromal cells. Primordial follicles were defined as small oocytes (<20 μm) surrounded by flat epithelial cells. Primary follicles were defined as having larger oocytes (>20 μm) surrounded by a single layer of cuboidal granulosa cells; secondary follicles were defined as larger oocytes surrounded by two or more layers of granulosa cells.

For immunohistochemistry, we used antibodies against GCNA1, MSY2, and SOHLH1 proteins. Anti-GCNA1 rat monoclonal antibody (11) was kindly provided by George C. Enders (University of Kansas, Kansas City), and anti-MSY2 rabbit immunoaffinity-purified antibody was kindly provided by Richard Schultz (University of Pennsylvania, Philadelphia). Polyclonal rabbit antibodies against SOHLH1 (COOH terminus; amino acids 121–357) were generated by using the pET-23 system (Novagen) and immunizing goats at Cocalico Biologicals (Reamstown, PA). The anti-SOHLH1 antibodies were immunoaffinity-purified over Affi-Gel 10 (Bio-Rad) and used in immunohistochemistry as described in ref. 20.

Microarray Analysis. Total RNA isolated from WT and *Sohlh1*$^{-/-}$ ovaries was used for oligonucleotide microarray analysis by using mouse genome 430 2.0 Array (Affymetrix, Santa Clara, CA) at the Baylor College of Medicine Microarray Core Facility with established protocols. Data were analyzed by using GENESPRING software (Silicon Graphics, Mountain View, CA).

RNA Isolation, RT-PCR, Quantitative Real-Time PCR, and *in Situ* Hybridization. Multitissue RT-PCR was performed as described in ref. 21. Oligonucleotides corresponding to *Sohlh1*, *Lhx8*, *Gdf9*, *Pou5f1*, and *Rfpl4* were selected by using PRIMER 3 software to generate an ≈500-bp nucleotide fragment that is interrupted by an intron within the mouse genome. The sequences of these primers are available on request from A.R. Mouse actin-specific primers were used to verify cDNA synthesis from RNA isolated from each tissue. PCR was carried out for 28 cycles on three independently collected pools of newborn ovaries.

Quantitative real-time PCR was performed on the Prism 7500 Sequence Detection System (Applied Biosystems) by using Assays-On-Demand PCR primer (Applied Biosystems) and probe sets for each gene and mouse *Gapd* (VIC-labeled MGD probe, primer limited, Applied Biosystems) as the endogenous control. RT-PCR was performed by using the TaqMan Universal PCR Master Mix (Applied Biosystems) in 20 μl. Each sample was analyzed in duplicate from at least three independent newborn WT and *Sohlh1*$^{-/-}$ cDNA samples. Two nontemplate control (RNase-free water) samples were included on each plate for each primer–probe set. The relative amount of transcript was calculated by the ΔΔCT method as described by Applied Biosystems by using 7500 SYSTEM 1.2.3 software (Applied Biosystems) and normalized to the endogenous reference (*Gapd*). One WT sample was randomly chosen to serve as the reference sample, to which all other samples were normalized. The average and standard error was calculated for the triplicate measurements, and the relative amount of target gene expression for each sample was plotted. Significance was performed by using Student's *t* test with EXCEL (Microsoft).

Mouse cDNA fragments corresponding to *Sohlh1*, *Lhx8*, *Zp1*, *Zp2*, *Zp3*, and *Figla* were subcloned into pGEM-T Easy vectors (Promega) and used to generate anti-sense and sense strands by labeling with [α-^{35}S]UTP using the Riboprobe T7/SP6 Combination System (Promega) (22). *In situ* hybridization was carried out as described in ref. 21. *In situ* hybridizations were performed on ovarian sections derived from two different animals.

Plasmids. Luciferase reporter vectors carrying mouse partial promoter sequences were constructed by introducing the PCR-amplified promoter into the vector of pGL4 (Promega). PCR amplification was performed by using oligonucleotides pLhx8-1 and pLhx8-2 for *Lhx8*, pNobox-1 and pNobox-2 for *Nobox*, pZp1-1 and pZp1-2 for *Zp1*, Zp2-1 and pZp2-2 for *Zp2*, and Zp3-1 and pZp3-2 for *Zp3* (Table 1, which is published as supporting information on the PNAS web site). To generate mutant E boxes, we used the QuikChange Multi Site-Directed Mutagenesis Kit (Stratagene) with the oligonucleotides listed in Table 1. An expression vector for mouse *Sohlh1* was constructed by cloning the full-length *Sohlh1* cDNA into pcDNA3 (Invitrogen).

Cell Culture and Reporter Assays. Human embryonic kidney cells (HEK293) were grown in DMEM with 10% FCS. For transient transfection, FuGENE6 (Roche Applied Science, Indianapolis) was used according to the manufacturer's instructions. After transfection, cells were cultured for 48 h before harvest. For each transfection, 200 ng of reporter construct, 200 ng of the indicated expression plasmid, and 20 ng of pRT-TK normalization plasmid (Promega) were used per well in a 12-well plate. Dual luciferase assays were carried out with total cell extracts as recommended by Promega. All transfection experiments were performed in triplicate, and results were normalized to the expression of *Renilla* luciferase. Data are relative to the mock transfection of empty parent vector, pGL4. Statistical analysis was performed by using one-way ANOVA followed by the Tukey–Kramer honestly significant difference test for multiple comparisons (JMP 5.1; JMP, Cary, NC). $P < 0.05$ was considered statistically significant.

ChIP. Mouse newborn ovaries and liver were collected and fixed directly in formaldehyde. The fixed ovaries were washed, homogenized, and prepared for immunoprecipitation by using a modified protocol of the ChIP assay kit (Upstate Biotechnology, Lake Placid, NY). The samples were precleared with salmon sperm DNA/protein A agarose (Upstate Biotechnology) and incubated with affinity-purified anti-SOHLH1 antibody or purified IgG at 4°C overnight. Chromatin samples immunoprecipitated by salmon sperm DNA/protein A agarose were washed two times with 1 ml of low-salt immune complex wash buffer (0.1% SDS/1% Triton X-100/2 mM EDTA/20 mM Tris·HCl, pH 8.1/150 mM NaCl), once with 1 ml of high-salt immune complex wash buffer (0.1% SDS/1% Triton X-100/2 mM EDTA/20 mM Tris·HCl, pH 8.1/500 mM NaCl), once with 1 ml of LiCl immune complex wash buffer (0.25 M LiCl/Igepal-CA630/1% sodium deoxycholate/1 mM EDTA/10 mM Tris·HCl, pH 8.1), and two times with 1 ml of TE buffer (10 mM Tris·HCl, pH 8.0/1 mM EDTA). Immune complexes were eluted from the antibody by adding 500 μl of elution buffer (0.1% SDS, 0.1M $NaHCO_3$). The complex-DNA cross-links were reversed by adding 20 μl of 5 M NaCl and heating at 65°C for 4 h and then adding 10 μl of 0.5 M EDTA, 20 μl of 1 M Tris·HCl (pH 6.5), and 2 μl of proteinase K (10 mg/ml) for 1 h at 45°C. DNA was recovered by phenol/chloroform extraction and ethanol precipitation, and redissolved in TE buffer. The supernatant of an immunoprecipitation reaction performed in the absence of the anti-SOHLH1 antibody was purified and used as a control. PCR analysis used primers from promoter regions of *Lhx8*, *Nobox*, *Zp1*, *Zp2*, or *Zp3*, shown in Table 2, which is published as supporting information on the PNAS web site.

This work was supported National Institutes of Health Grant HD44858 and March of Dimes Basil O'Connor Award 5-FY02-266 (to A.R.), National Institutes of Health Grant HD42500 (to M.M.M.), and National Institutes of Health/National Research Service Award 5F32 HD46335-01A1 (to S.A.P.).

1. Pepling, M. E. & Spradling, A. C. (2001) *Dev. Biol.* **234,** 339–351.
2. Wylie, C. (1999) *Cell* **96,** 165–174.
3. Rajkovic, A., Pangas, S. A., Ballow, D., Suzumori, N. & Matzuk, M. M. (2004) *Science* **305,** 1157–1159.
4. Dong, J., Albertini, D. F., Nishimori, K., Kumar, T. R., Lu, N. & Matzuk, M. M. (1996) *Nature* **383,** 531–535.
5. Dean, J. (2002) *J. Reprod. Immunol.* **53,** 171–180.
6. Elvin, J. A., Yan, C. & Matzuk, M. M. (2000) *Mol. Cell. Endocrinol.* **159,** 1–5.
7. Soyal, S. M., Amleh, A. & Dean, J. (2000) *Development (Cambridge, U.K.)* **127,** 4645–4654.
8. Liang, L., Soyal, S. M. & Dean, J. (1997) *Development (Cambridge, U.K.)* **124,** 4939–4947.
9. Suzumori, N., Yan, C., Matzuk, M. & Rajkovic, A. (2001) *Mech. Dev.* **111,** 137–141.
10. Ballow, D., Meistrich, M., Matzuk, M. & Rajkovic, A. (2006) *Dev. Biol.*, in press.
11. Enders, G. C. & May, J. J., II (1994) *Dev. Biol.* **163,** 331–340.
12. Gu, W., Tekur, S., Reinbold, R., Eppig, J. J., Choi, Y. C., Zheng, J. Z., Murray, M. T. & Hecht, N. B. (1998) *Biol. Reprod.* **59,** 1266–1274.
13. Yu, J., Hecht, N. B. & Schultz, R. M. (2001) *Biol. Reprod.* **65,** 1260–1270.
14. Menke, D. B., Koubova, J. & Page, D. C. (2003) *Dev. Biol.* **262,** 303–312.
15. Mori, T., Yuxing, Z., Takaki, H., Takeuchi, M., Iseki, K., Hagino, S., Kitanaka, J., Takemura, M., Misawa, H., Ikawa, M., *et al.* (2004) *Eur. J. Neurosci.* **19,** 3129–3141.
16. Zhao, Y., Marin, O., Hermesz, E., Powell, A., Flames, N., Palkovits, M., Rubenstein, J. L. & Westphal, H. (2003) *Proc. Natl. Acad. Sci. USA* **100,** 9005–9010.
17. Zhao, Y., Guo, Y. J., Tomac, A. C., Taylor, N. R., Grinberg, A., Lee, E. J., Huang, S. & Westphal, H. (1999) *Proc. Natl. Acad. Sci. USA* **96,** 15002–15006.
18. Simpson, J. L. & Rajkovic, A. (1999) *Am. J. Med. Genet.* **89,** 186–200.
19. Zhang, H., Hasty, P. & Bradley, A. (1994) *Mol. Cell. Biol.* **14,** 2404–2410.
20. Pangas, S. A., Rademaker, A. W., Fishman, D. A. & Woodruff, T. K. (2002) *J. Clin. Endocrinol. Metab.* **87,** 2644–2657.
21. Rajkovic, A., Yan, M. S. C., Klysik, M. & Matzuk, M. (2001) *Fertil. Steril.* **76,** 550–554.
22. Albrecht, U., Eichele, G., Helms, J. A. & Lu, H. C. (1997) in *Molecular and Cellular Methods in Developmental Toxicology*, ed. Daston, G. P. (CRC, Boca Raton, FL), pp. 23–48.